

# Mapping Mining Expansion in the Aprampama Forest Reserve with Low-Shot Learning and Satellite Embeddings

Richmond Akwasi NSIAH, Ghana, Prosper Basommi LAARI, Ghana, and Qingfeng GUAN, China

**Key words:** mining, forest reserve, land cover, classification, embedding

## SUMMARY

The rapid expansion of artisanal and small-scale mining (ASM) within ecologically sensitive forest reserves in Ghana has contributed significantly to land use and land cover (LULC) changes. Monitoring these dynamics remains challenging due to cloud interference, spectral confusion, and the absence of high-quality labelled data. This study applies a machine learning classification approach using the AlphaEarth Foundations (AEF) satellite embedding dataset to map and assess mining activity in the Apamprama Forest Reserve from 2017 to 2024. Sentinel-2 median composites were used to generate ground control points (GCPs), while AEF embeddings enabled low-shot classification into mining, vegetation, and water classes. A Random Forest classifier was trained annually and evaluated using both internal validation and post-classification assessments with independent ground truth data from Google Earth Pro. Results show a progressive expansion of mining from 0.1 km<sup>2</sup> in 2017 to over 12 km<sup>2</sup> in 2024, accompanied by a significant decline in vegetation. Classification accuracy exceeded 90% across most years, although some misclassifications occurred due to sedimentation and regrowth in abandoned pits. The findings provide spatial insights into the spiralling of mining activities within a protected ecosystem and underscore the effectiveness of pre-trained geospatial embeddings for environmental monitoring. This research can support timely detection and informed policy intervention in tropical regions.

# Mapping Mining Expansion in the Aprampama Forest Reserve with Low-Shot Learning and Satellite Embeddings

Richmond Akwasi NSIAH, Ghana, Prosper Basommi LAARI, Ghana, and Qingfeng GUAN, China

## 1. INTRODUCTION

The Earth's surface and ecosystems are undergoing rapid changes driven mainly by anthropogenic factors, with mining operations, particularly artisanal and small-scale mining (ASM), being a significant contributor to land use and land cover (LULC) modifications globally (Djaba and Djaba, 2023; Forkuor *et al.*, 2020). In Ghana, this issue is particularly acute, as the country's rainforest is experiencing some of the world's fastest deforestation rates, with mining identified as a primary driver alongside agriculture, logging, fires, and urban expansion (Gallwey *et al.*, 2020). The environmental repercussions of mining are profound, encompassing extensive destruction of natural vegetation and farmland, soil removal, expansion of bare soil surfaces, and vulnerability to land degradation and erosion (Mhangara *et al.*, 2020; Musiałek and Maksymowicz, 2025). Furthermore, these activities are a significant source of water pollution (e.g., river siltation, mercury and cyanide contamination, heavy metal release), air pollution (dust, smoke), and direct destruction of wildlife habitats, threatening biodiversity (Ammirati *et al.*, 2020; Moomen *et al.*, 2022; Myroniuk *et al.*, 2020). Given these pervasive and often severe impacts, accurate, timely, and efficient monitoring of mining activities is crucial for understanding, limiting, and mitigating their negative consequences, thereby supporting sustainable development and conservation efforts (Forkuor *et al.*, 2020; Matingo, 2023; Musiałek and Maksymowicz, 2025).

Despite the critical need for robust monitoring, tracking mining activities, especially illegal and informal operations that are often remote and clandestine, presents substantial challenges for traditional Earth Observation (EO) approaches (Adamek *et al.*, 2021; Elmes *et al.*, 2014). These difficulties stem from several factors: persistent cloud cover in tropical regions frequently limits the availability of usable optical images, hindering consistent observation (Djaba and Djaba, 2023; Snapir *et al.*, 2017). Spectral similarities between bare soil surfaces and excavated pits can lead to misclassification, making accurate mapping difficult. Moreover, small-scale and diffuse mining sites, often characterised by mixed pixels, are challenging to detect with moderate spatial resolution imagery (Koziońska and Górnjak-Zimroz, 2021; Wang *et al.*, 2020). Beyond technical limitations, traditional EO methods often rely on extensive, high-quality labelled datasets for training, which are scarce due to the significant effort and resources required for ground-based measurements and annotations. This scarcity of reliable labels, coupled with the computational demands of processing petabytes of satellite imagery for

planetary-scale insights, hampers the ability to produce timely and accurate maps for effective environmental management (Brown *et al.*, 2025).

To address these limitations, this research proposes to leverage the AlphaEarth Foundations (AEF) dataset to monitor mining activities within the Aprampama Forest Reserve in Ghana from 2017 to 2024. Specifically, this study aims to harness AEF's scalable, low-shot learning capabilities to accurately map the spatial distribution and temporal dynamics of mining-induced land cover changes and deforestation within the Aprampama Forest Reserve, providing critical insights into the scale and patterns of environmental degradation. This research holds significant promise for enhancing conservation and sustainable development, informing policy, improving land management, and targeting interventions against illegal mining.

## 2. LITERATURE REVIEW AND GAPS

Despite the wide range of existing methods designed to monitor mining activities within forest reserves, significant limitations continue to impede their effectiveness. To begin with, persistent cloud cover poses a formidable obstacle for optical imagery, particularly in tropical mining regions such as Ghana, where frequent overcast conditions severely hinder consistent observation over time (Forkuor *et al.*, 2020). Synthetic Aperture Radar (SAR) data offers a viable alternative means to address this challenge by penetrating cloud cover. However, it is susceptible to vegetation coverage and may affect its performance in identifying artisanal mines within forest reserves (Nursamsi *et al.*, 2024). Furthermore, the spectral similarity between bare soil and excavated pits remains a persistent challenge, frequently leading to misclassification errors in traditional pixel-based classification methods (Delaney *et al.*, 2025).

Besides, the diffused and small-scale nature of numerous artisanal mining activities results in mixed pixels. This phenomenon can complicate detection efforts when using conventional classification techniques that rely on moderate-resolution imagery (Fonseca *et al.*, 2024). Furthermore, approaches incorporating advanced machine learning techniques, especially deep-learning models, require substantial volumes of high-quality, labelled training data to achieve reliable performance (Couttenier *et al.*, 2022). However, acquiring comprehensive and accurate ground-based labels is a daunting task, as it is not only time-consuming and labour-intensive but also logistically challenging and poses safety risks, particularly when targeting illegal and remotely located mining sites (Chike and Balz, 2024). This scarcity of reliable labels subsequently restricts the scalability and generalisability of these models across diverse geographical regions and varying operational contexts (Shivashankar *et al.*, 2025).

Another challenge is the processing of petabytes of satellite imagery for large-scale or global monitoring efforts using traditional methods. This process is computationally demanding and resource-intensive, often straining existing infrastructure and delaying the delivery of

actionable insights (Dritsas and Trigka, 2025). Collectively, these limitations emphasise the need for innovative solutions that can overcome data scarcity, enhance detection accuracy, and streamline processing to support effective environmental management in mining-affected forest reserves.

The AlphaEarth Foundations (AEF) dataset presents an innovative solution to address the challenges of data scarcity and computational efficiency in monitoring mining activities. It introduces a novel embedding field model that integrates spatial, temporal, and measurement contexts from diverse EO sources, transforming raw data into analysis-ready embedding layers tailored for a variety of mapping and monitoring tasks (Brown *et al.*, 2025). AEF excels in low-shot learning, outperforming existing featurisation methods across land use/land cover mapping and change detection tasks without retraining, demonstrating strong generalisation with minimal training samples. The dataset provides temporally consistent annual embedding fields from 2017 to 2024 at a 10-meter resolution, leveraging inputs like Sentinel-1 SAR and Sentinel-2 optical data for robust time-series analysis. Additionally, AEF enhances efficiency and scalability by offering a pre-trained, general-purpose geospatial representation, reducing the computational burden and human effort required for large-scale monitoring, thereby facilitating informed decision-making and policy development on a global scale.

### 3. MATERIALS AND METHODS USED

#### 3.1. Study Area

The Apamprama Forest Reserve is one of the four designated forest reserves situated within the Amansie Central and Amansie West Districts of the Ashanti Region, as depicted in Figure 1. This protected area encompasses approximately 36.28 km<sup>2</sup> and is geographically positioned between latitudes 06° 22' 08" N and 06° 17' 14" N, and longitudes 01° 55' 16" W and 01° 48' 21" W. The encompassing districts, located in the southwestern sector of the Ashanti Region, collectively span a vast land area of about 2074 km<sup>2</sup>. These districts are characterised by predominantly undulating plateaus, with elevations ranging from 150 meters to 300 meters above sea level, contributing to a diverse topography that influences local ecosystems and land use patterns (Mantey and Otoo, 2020).

The climate within this region is classified as semi-equatorial and wet, fostering a rich ecological environment. This climate is marked by an average annual rainfall of approximately 1700 mm, which supports the lush vegetation typical of forest reserves in this zone. Temperatures in the area fluctuate between 20 °C and 32 °C throughout the year, creating a warm and humid setting conducive to a variety of flora and fauna. The forest is notably drained by the River Offin, a significant waterway that plays a crucial role in the hydrological system of the reserve, influencing water availability and supporting the biodiversity that thrives within

its boundaries. This geographical and climatic context underscores the reserve's importance as a critical ecological zone, particularly in the face of pressures such as mining activities that threaten its integrity (Mantey and Otoo, 2020).

Moreover, beyond its local ecological importance, the Apampama Forest Reserve represents a broader class of protected forest landscapes in Ghana that are increasingly exposed to artisanal and small-scale mining pressures. Its selection reflects both its protected status and documented mining encroachment, making it an appropriate test site for evaluating monitoring approaches under persistent cloud cover, limited ground-truth data, and rapid land disturbance. Similar pressures have been reported in other forest reserves across Ghana's forest belt, suggesting that the spatial patterns observed in this study may reflect broader national trends.

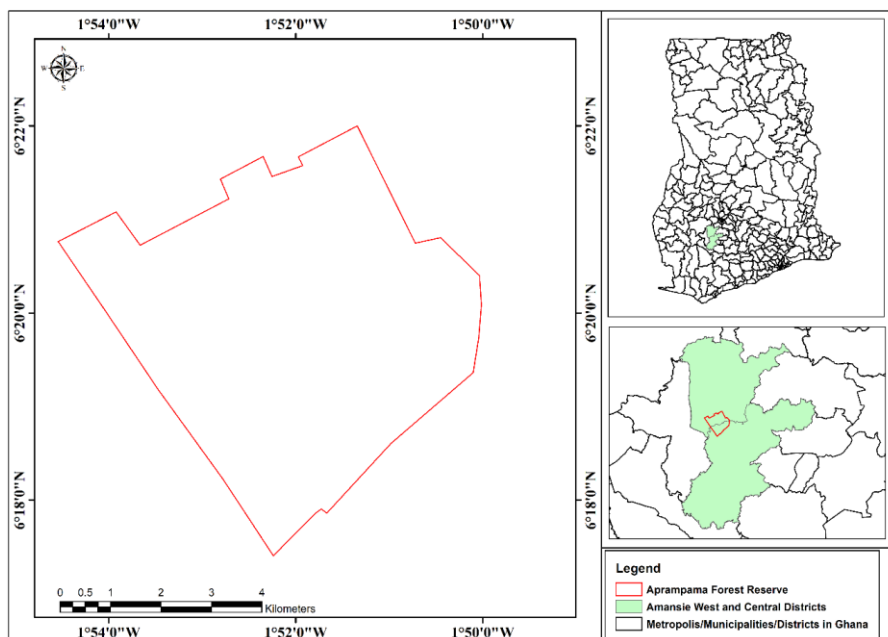


**Figure 1: Map of the Study Area (The upper-right inset depicts the entire territory of Ghana).**

**Source: Author's Construct**

### 3.2 Datasets

This study employs two primary datasets—the Sentinel-2 Surface Reflectance Harmonised dataset and the AlphaEarth Foundations (AEF) Satellite Embedding dataset, both of which were accessed via Google Earth Engine (GEE).

The Sentinel-2 Surface Reflectance Harmonised dataset, provided by the European Space Agency (ESA), is a global collection of Level-2A products featuring 13 spectral bands at spatial

resolutions of 10m, 20m, and 60m. This dataset includes visible, near-infrared (NIR), and shortwave infrared (SWIR) bands, with a revisit time of approximately 5 days due to the twin-satellite constellation. For this study, the dataset was utilised to generate annual median composites for each year from 2017 to 2024, covering the Apamprama Forest Reserve. The imagery was filtered by a temporal range from 1 January to 31 December of each year and spatially constrained to the study area. A cloud masking procedure was applied using the GOOGLE/CLOUD\_SCORE\_PLUS/V1/S2\_HARMONIZED collection to mitigate cloud contamination. This procedure was performed by linking cloud score (cs) data to Sentinel-2 images and retaining only pixels with a 'cs' band value  $\geq 0.6$ . The resulting cloud-masked collection was processed into a median composite, visualised in false colour (using SWIR band B11, NIR band B8, and red band B4) to emphasise land cover differences. The outcome of the false colour composite for each year was used for initial visual assessment and ground control point (GCP) selection.

The AlphaEarth Foundations (AEF) Satellite Embedding dataset, developed by Google DeepMind, was accessed via GOOGLE/SATELLITE\_EMBEDDING/V1/ANNUAL on Google Earth Engine. This dataset offers a pre-trained, high-dimensional geospatial representation derived from a diverse array of Earth observation (EO) sources, including Sentinel-1 SAR and Sentinel-2 optical data. This dataset provides annual embedding fields at a 10-meter resolution from 2017 to 2024, designed for low-shot learning and general-purpose mapping tasks without requiring extensive retraining. The embeddings integrate spatial, temporal, and measurement contexts, transforming raw EO data into analysis-ready layers that support applications such as land use/land cover classification and change detection. In this study, the AEF dataset was utilised by filtering the image collection for each year's temporal range (1 January to 31 December) and the study area bounds, followed by mosaicking to create a single annual embedding image. This image served as the data source for classifying the study area into mining, water, or vegetation.

### 3.3 Methodology

This study employed a satellite-based classification framework to monitor land cover dynamics—specifically mining, vegetation, and water—within the Apamprama Forest Reserve over an eight-year period (2017–2024). The process, depicted in Figure 2, involved image preprocessing, ground control point (GCP) creation, land cover classification using satellite embeddings, and post-classification analysis. All satellite data processing and classification tasks were conducted using Google Earth Engine (GEE), with spatial quantification performed in ArcMap.

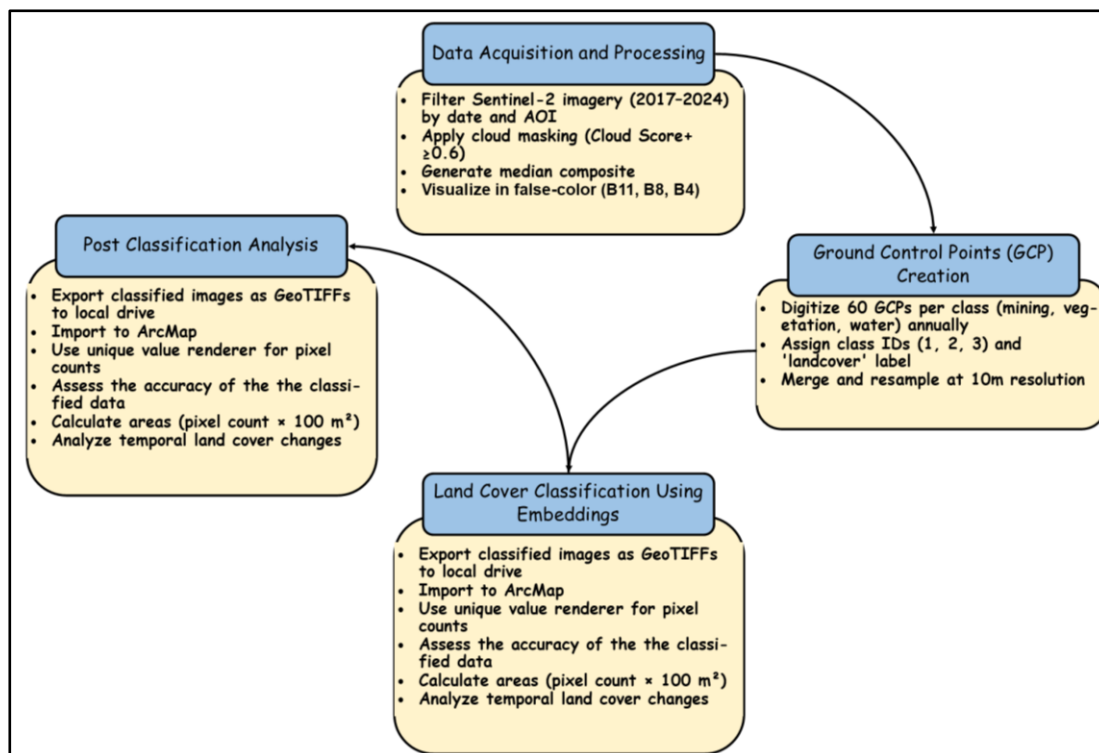


**Figure 2: Methodological Workflow**

### 3.3.1 Data Acquisition and Preprocessing

Annual median composites of Sentinel-2 imagery were generated by filtering the imagery by calendar year (1 January to 31 December) and clipping to the forest reserve boundary. To enhance the usability of the imagery, a cloud masking algorithm was applied using the Google Cloud Score+ dataset. Pixels with a cloud score (cs)  $\geq 0.6$  were retained, and the cloud-free images were composited using the median reducer. The resulting composites were visualised in a false-colour scheme using the SWIR (B11), NIR (B8), and Red (B4) bands. This configuration enhances the contrast between vegetation, bare earth, and water bodies, facilitating land cover identification and visual assessment.

### 3.3.2 Ground Control Point (GCP) Creation

Representative ground control points (GCPs) for mining, vegetation, and water classes were manually digitised within the GEE environment using the geometry tool. Each GCP was created as a feature collection with two attribute fields: a class identifier ('1' for mining, '2' for vegetation, and '3' for water) and a property label 'landcover'.

For each year from 2017 to 2024, a total of 60 GCPs were created for each class (mining, vegetation, water), yielding a balanced training dataset of 180 GCPs per year. These points were identified based on expert visual interpretation of the false-colour Sentinel-2 composites. The

individual GCP feature collections were merged into a single collection and resampled at 10-meter resolution to match the spatial scale of the input imagery.

### 3.3.3 Land Cover Classification Using Embeddings

Land cover classification was conducted using the AlphaEarth Foundations (AEF) Satellite Embedding dataset. For each year, the AEF image collection was filtered by date and spatially bounded to the study area, then mosaicked into a single annual image. The merged GCP feature collection was overlaid on the annual embedding image using the 'sampleRegions' function to extract spectral embedding vectors associated with each class. The sample dataset was randomly split into training (80%) and validation (20%) subsets based on a random value column.

A Random Forest classifier with 50 decision trees was trained on the embedding vectors, using the 'landcover' attribute as the target label. Model accuracy was assessed by computing a confusion matrix comparing predicted and actual labels in the validation subset. The confusion matrix was subsequently used to derive standard performance metrics, including overall accuracy (OA), precision, recall, and the F1-1 score. Overall accuracy computes the proportion of correctly classified pixels across all classes. Precision evaluates the ratio of true positives to the sum of true and false positives, while recall assesses the ratio of true positives to the sum of true positives and false negatives. F1-score, on the other hand, is the harmonic mean of precision and recall. These metrics were calculated annually to ensure temporal consistency and to identify any variations in classification reliability over the eight-year study period. The trained model was applied to each year's embedding mosaic to generate a classified image with land cover values assigned as follows: 1 = mining, 2 = vegetation, 3 = water. A colour palette was applied to visualise the final classified images, and subsequently they were clipped to the study area's boundary for export and further analysis.

### 3.3.4 Post-Classification Analysis

Each classified image was exported from GEE to a local drive as a GeoTIFF file using the 'Export.image.toDrive' function. The classified rasters were imported into ArcMap, where a unique value renderer was used to identify the pixel count for each land cover class. A post-classification assessment was subsequently conducted using independent reference data to validate the accuracy of the classified data for 2019 and 2024, as the high-resolution imagery for the study area was available for these years. For the years considered, 25 validation samples were manually collected for each land cover class (mining, vegetation, and water), yielding 75 independent samples for each of these years. These samples were obtained through visual inspection and interpretation of high-resolution imagery in Google Earth Pro. The reference points were then overlaid on the classified images in ArcMap to verify the correctness of the assigned land cover class.

To compute the spatial extent of each land cover class, the respective pixel counts obtained for each land cover class were multiplied by 100 m<sup>2</sup>, reflecting the 10 m × 10 m resolution of the imagery. This computation enabled temporal analysis of annual land cover change, particularly the expansion of mining activity within the Apamprama Forest Reserve.

**4. RESULTS AND DISCUSSION**

This section evaluates the spatial and temporal evolution of mining activity within the Apamprama Forest Reserve using annual classified maps from 2017 to 2024. The discussion is structured into four parts: assessment of the training performance of the classifier, post-classification validation using ground truth data, analysis of annual mining extent, and interpretation of land cover change maps.

**4.1 Training Accuracy**

Table 1 summarises the annual performance metrics, accuracy, precision, recall, and F1-score of the classifier trained using geospatial satellite embedding datasets. The classifier demonstrated excellent performance in 2017, 2018, and 2021, with all metrics approaching or reaching 0.999. Moderate classification performance was observed in 2019, 2022, and 2024, while the lowest performance was recorded in 2020 and 2023. This decline could be attributed to factors such as spectral confusion between mining areas and water bodies due to sediment-laden runoff or the presence of vegetated regrowth in abandoned mine pits being misclassified as forest. Nevertheless, the model maintained a high overall performance across the years, with most evaluation scores exceeding 90%. Figure 3 depicts the annual training performance metrics.

**Table 1: Annual Training Performance for Machine Learning Classifier**

<b>Year</b>	<b>Accuracy</b>	<b>Precision</b>	<b>Recall</b>	<b>F1-Score</b>
<b>2017</b>	0.999	0.999	0.999	0.999
<b>2018</b>	0.999	0.999	0.999	0.999
<b>2019</b>	0.977	0.971	0.974	0.971
<b>2020</b>	0.906	0.906	0.904	0.904
<b>2021</b>	0.999	0.999	0.999	0.999
<b>2022</b>	0.925	0.928	0.922	0.924
<b>2023</b>	0.900	0.921	0.892	0.898
<b>2024</b>	0.974	0.974	0.972	0.973

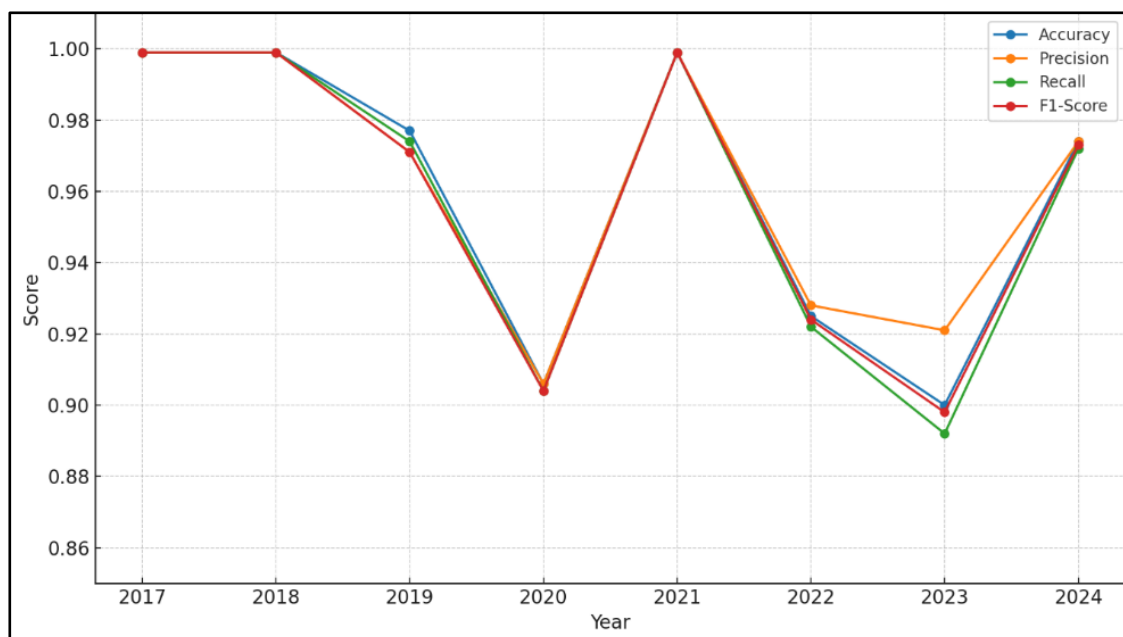


**Figure 3: Training Metrics (2017-2018)**

#### 4.2 Post Classification Assessment

A post-classification validation was conducted for 2019 and 2024 using independent samples derived from Google Earth Pro. As shown in Table 2, both years exhibited a decrease in performance compared to training metrics. For 2019, the model achieved an accuracy of 0.907, F1-score of 0.905, and recall of 0.916, indicating effective detection of actual land cover classes, albeit with some false positives. A similar trend was observed in 2024, with slightly lower accuracy (0.893) and precision (0.889). The reduction in precision suggests misclassification between mining and other spectrally similar classes or vice versa. Despite these discrepancies, the classifier's performance remained robust and acceptable for land use/land cover monitoring. Figure 4 depicts the post-classification assessment for 2019 and 2024.

**Table 2: Post-Classification Assessment for 2019 and 2024**

	2019	2024
<b>Metric</b>	<b>Value</b>	
Accuracy	0.907	0.893
Precision (Macro)	0.914	0.889
Recall (Macro)	0.916	0.909
F1-Score (Macro)	0.905	0.891

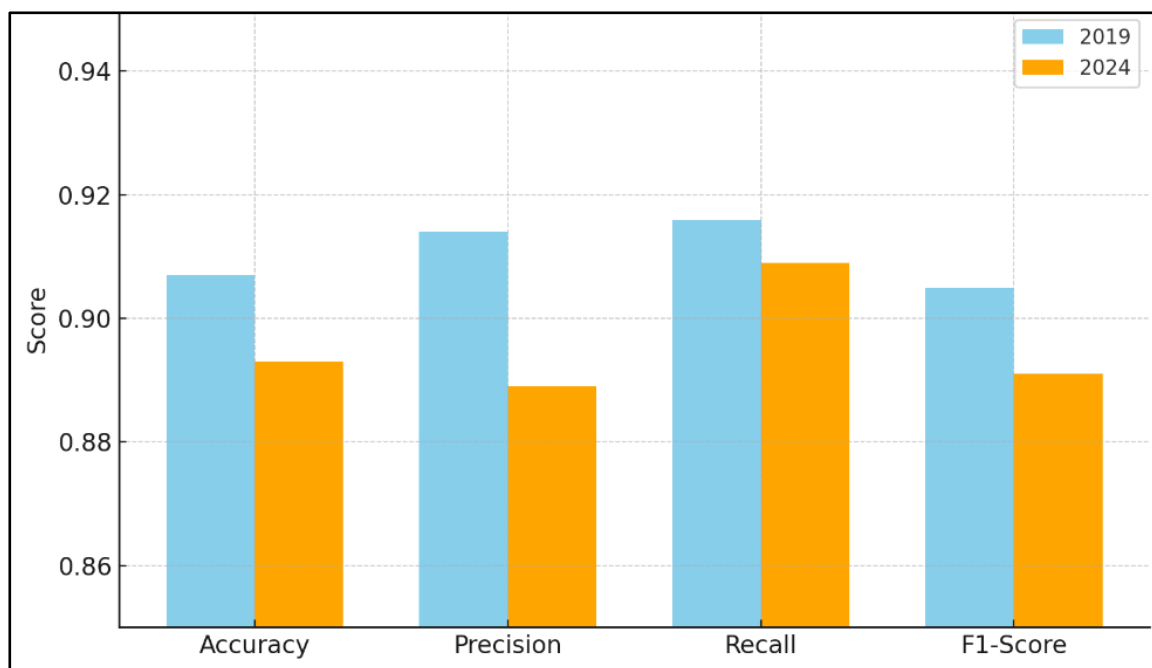


**Figure 4: Post-Classification Assessment for 2019 and 2024**

### 4.3 Temporal Analysis of Mining Extent

The areal extent of each land cover class—mining, vegetation, and water—was computed annually from the classified images. Table 3 shows that mining activities were almost negligible in 2017, occupying only 101,400 m<sup>2</sup>. However, from 2018 onward, a steady and significant increase in mining area is observed, expanding to 12,157,100 m<sup>2</sup> by 2024. This trend indicates progressive encroachment of mining into forested areas, especially along riverbanks and near previously mined zones. Concurrently, vegetation cover declined from 36.8 million m<sup>2</sup> in 2017 to 22.5 million m<sup>2</sup> in 2024, suggesting substantial forest degradation. The area covered by water bodies also fluctuated, increasing from 671,600 m<sup>2</sup> in 2017 to nearly 3 million m<sup>2</sup> in 2024, potentially due to sedimentation, pit lakes, or re-channelling caused by mining activities. Figure 5 visually depicts the computed annual coverage for each land cover class.

**Table 3: Computed Annual Land Cover Coverage**

Year	Class	Area (m <sup>2</sup> )
2017	Mining	101400
	Vegetation	36842900
	Water	671600
2018	Mining	3147900
	Vegetation	33667600
	Water	800400

2019	Mining	3058600
	Vegetation	33494500
	Water	1062800
2020	Mining	6518000
	Vegetation	30425000
	Water	672900
2021	Mining	9440900
	Vegetation	26057000
	Water	2118000
2022	Mining	10919700
	Vegetation	24719600
	Water	1976600
2023	Mining	10551600
	Vegetation	24553800
	Water	2510500
2024	Mining	12157100
	Vegetation	22463900
	Water	2994900

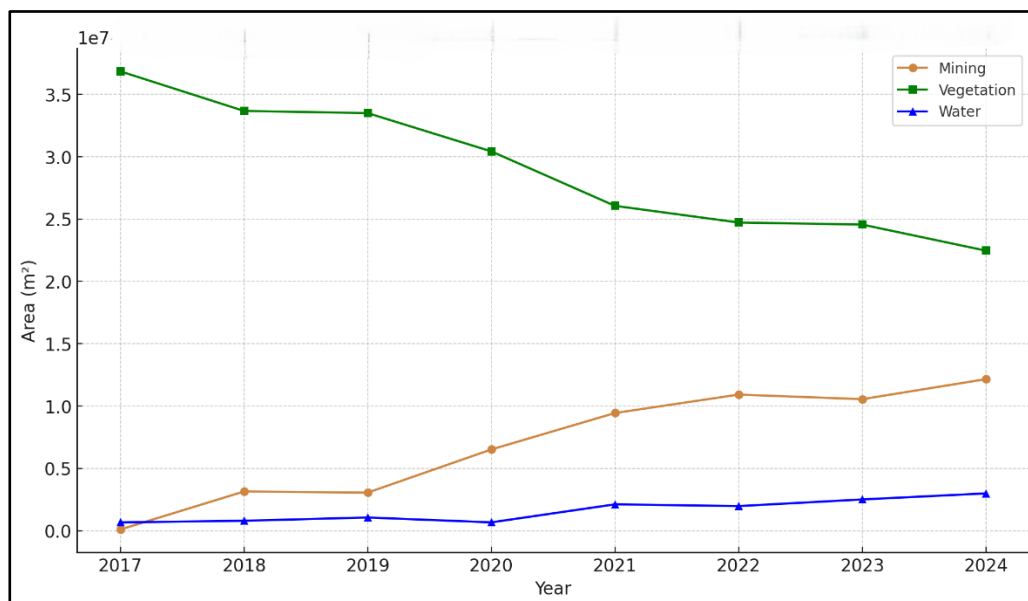


**Figure 5: Annual Land Cover Area within the Aprampama Forest Reserve**

#### 4.4 Classified Maps

Figures 6 to 13 illustrate the spatial distribution of land cover classes for each year. In 2017 (Figure 6), the reserve is overwhelmingly vegetated, with minimal mining activity concentrated

near the southwestern boundary. From 2018 (Figure 7), mining footprints begin to emerge along river channels, and by 2020 (Figure 9), considerable fragmentation of vegetation is evident. The peak of mining activity is visualised in the 2024 map (Figure 13), where mining dominates the central and northeastern parts of the reserve, forming dense clusters and linear expansions that follow hydrological features.

These visualisations confirm the results of the areal computations and emphasise the growing threat of mining activities to the ecological integrity of the Apamprama Forest Reserve.

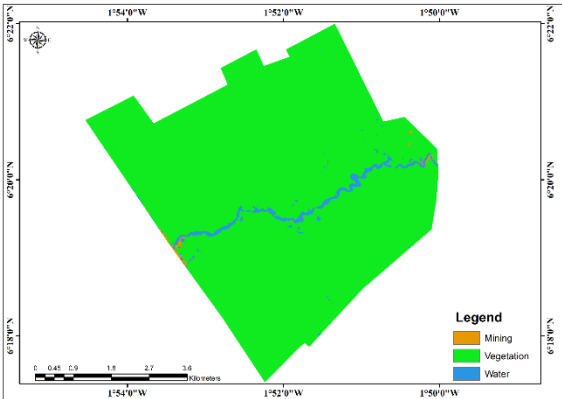


**Figure 6: LULC for 2017**

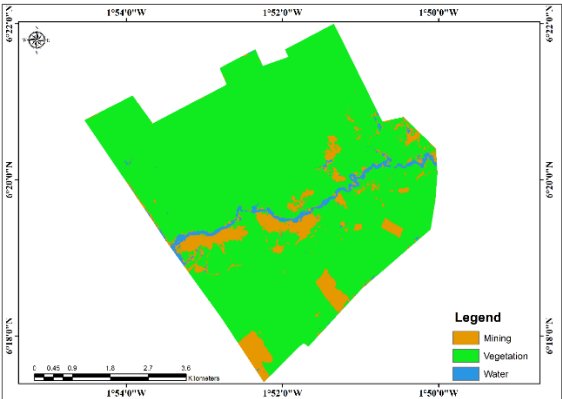


**Figure 7: LULC for 2018**

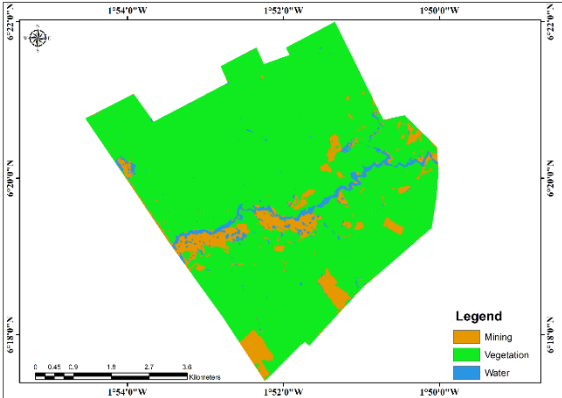


**Figure 8: LULC for 2019**

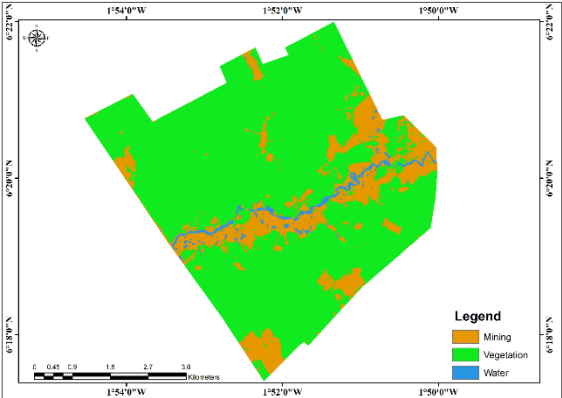


**Figure 9: LULC for 2020**

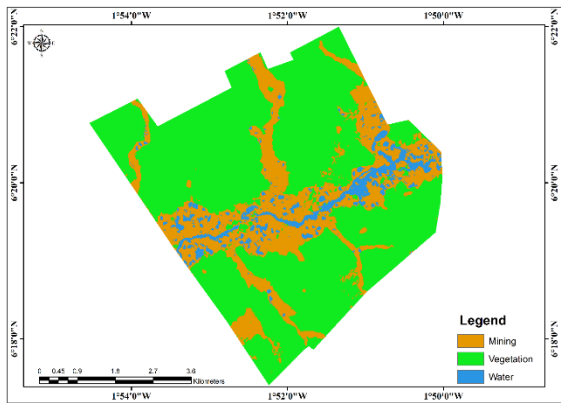


**Figure 10: LULC for 2021**

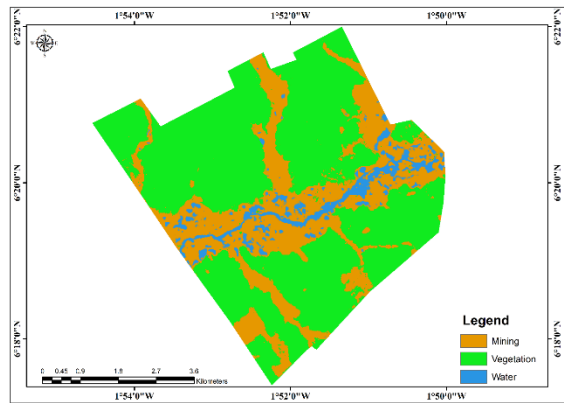


**Figure 11: LULC for 2022**

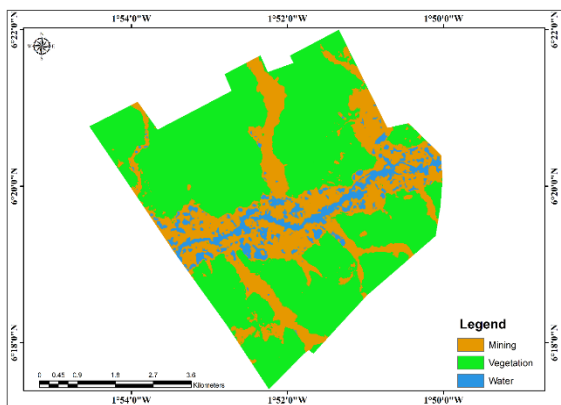


**Figure 12: LULC for 2023**

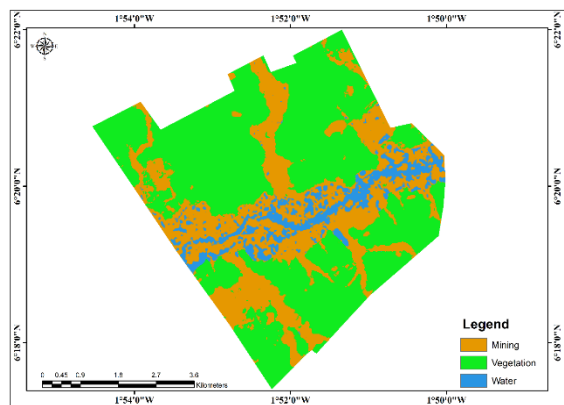


**Figure 13: LULC for 2024**

#### 4.5 Discussion

The findings of this study reveal distinct spatial and temporal patterns of increasing mining activity within the Apamprama Forest Reserve. The use of AlphaEarth Foundations (AEF) embeddings significantly enhanced classification accuracy, enabling reliable detection of mining, vegetation, and water classes across a diverse landscape. A notable trend observed was that while mining activity was minimal in 2017, it expanded rapidly from 2018 onwards, reaching over 12 km<sup>2</sup> by 2024, a more than 100-fold increase in area. This expansion correlates with visible landscape fragmentation, particularly along riverbanks, which are known hotspots for ASM.

Moreover, the classification framework proved robust, with training accuracy metrics consistently above 90% and F1-scores approaching perfect performance in optimal years. Nevertheless, performance variability was evident, especially in 2020 and 2023, where spectral overlap likely contributed to lower precision. The presence of sediments in water bodies or vegetative regrowth in inactive pits is a challenge in traditional pixel-based classification methods. Post-classification validation established that recall remained high, indicating the

model successfully detected most mining locations. Conversely, precision decreased slightly due to the inclusion of false positives.

The observed increase in water coverage also suggests hydrological alterations, potentially from pit lakes, re-channelling, or sediment deposition, indicating broader environmental consequences beyond deforestation. These results demonstrate the applicability of AEF in low-label environments and its value in high-frequency monitoring of mining impacts in conservation areas.

## **5. CONCLUSION AND RECOMMENDATIONS**

### **5.1 Conclusion**

This study demonstrates the efficacy of using AlphaEarth Foundations (AEF) satellite embeddings and machine learning classification to map and monitor mining activity within Ghana's Apamprama Forest Reserve. Over the eight years from 2017 to 2024, mining activity expanded significantly, accompanied by a marked decline in forest cover and increases in water surface area. The use of low-shot learning with AEF embeddings enabled accurate land cover classification even with limited ground truth data, highlighting the potential for scalable, cost-effective environmental monitoring. The visual and quantitative results confirm that mining activities (possibly artisanal and small-scale and industrial mining) have encroached into the forest reserve, contributing to extensive land degradation. These insights are crucial for regulatory agencies and conservation planners in enforcing land use policies and initiating ecological restoration efforts.

Although this analysis focuses on the Apamprama Forest Reserve, illegal and informal mining activities are widespread across Ghana's forest reserves and river basins. The low-shot, embedding-based monitoring framework demonstrated in this study is highly transferable and can support near-real-time detection, prioritisation of enforcement actions, and consistent national reporting. This highlights the growing role of foundation-model-based artificial intelligence in counteracting environmental degradation and strengthening forest governance in tropical regions.

### **5.2 Recommendations**

Based on the results obtained, the study recommends that:

1. National agencies and regulatory bodies such as the Environmental Protection Agency (EPA) and Forestry Commission (FC) adopt the pre-trained embeddings and AI-powered dashboards for real-time monitoring of mining footprints.
2. The identified hotspots of degradation should be prioritised for reforestation and ecological restoration, particularly along waterways and areas of high biodiversity.

3. Sustainable mining practices and community-based monitoring initiatives should be promoted among local populations to balance livelihoods and conservation goals.

## REFERENCES

- Adamek, K., Lupa, M. and Zawadzki, M. (2021), "Remote sensing techniques for tracking changes caused by illegal gold mining in Madre de Dios, Peru", *Miscellanea Geographica*, Vol. 25 No. 4, pp. 205–212, doi: 10.2478/mgrsd-2020-0028.
- Ammirati, L., Mondillo, N., Rodas, R.A., Sellers, C. and Di Martire, D. (2020), "Monitoring Land Surface Deformation Associated with Gold Artisanal Mining in the Zaruma City (Ecuador)", *Remote Sensing*, Vol. 12 No. 13, p. 2135, doi: 10.3390/rs12132135.
- Brown, C.F., Kazmierski, M.R., Pasquarella, V.J., Rucklidge, W.J., Samsikova, M., Zhang, C., Shelhamer, E., *et al.* (2025), "AlphaEarth Foundations: An embedding field model for accurate and efficient global mapping from sparse label data", arXiv, 29 July, doi: 10.48550/arXiv.2507.22291.
- Chike, I. and Balz, T. (2024), "Detecting and Monitoring Artisanal Mining Operations in Semi-Arid Terrain Using Multitemporal SAR Data for InSAR Coherence Estimation and Unsupervised Classification", *The International Archives of the Photogrammetry, Remote Sensing and Spatial Information Sciences*, Vol. XLVIII-1–2024, pp. 105–110, doi: 10.5194/isprs-archives-XLVIII-1-2024-105-2024.
- Couttenier, M., Di Rollo, S., Inguere, L., Mohand, M. and Schmidt, L. (2022), "Mapping artisanal and small-scale mines at large scale from space with deep learning", *PLOS ONE*, Public Library of Science, Vol. 17 No. 9, pp. 1–13, doi: 10.1371/journal.pone.0267963.
- Delaney, B., Tansey, K. and Whelan, M. (2025), "Satellite Remote Sensing Techniques and Limitations for Identifying Bare Soil", *Remote Sensing*, Vol. 17 No. 4, doi: 10.3390/rs17040630.
- Djaba, P. and Djaba, S. (2023), "A GEOSPATIAL APPROACH IN RESOLVING ILLEGAL MINING ACTIVITIES IN GHANA".
- Dritsas, E. and Trigka, M. (2025), "Remote Sensing and Geospatial Analysis in the Big Data Era: A Survey", *Remote Sensing*, Vol. 17 No. 3, doi: 10.3390/rs17030550.
- Elmes, A., Yarlequé Ipanaqué, J.G., Rogan, J., Cuba, N. and Bebbington, A. (2014), "Mapping licit and illicit mining activity in the Madre de Dios region of Peru", *Remote Sensing Letters*, Vol. 5 No. 10, pp. 882–891, doi: 10.1080/2150704X.2014.973080.
- Fonseca, A., Marshall, M.T. and Salama, S. (2024), "Enhanced Detection of Artisanal Small-Scale Mining with Spectral and Textural Segmentation of Landsat Time Series", *Remote Sensing*, Vol. 16 No. 10, doi: 10.3390/rs16101749.
- Forkuor, G., Ullmann, T. and Griesbeck, M. (2020), "Mapping and Monitoring Small-Scale Mining Activities in Ghana using Sentinel-1 Time Series (2015–2019)", *Remote Sensing*, Vol. 12 No. 6, p. 911, doi: 10.3390/rs12060911.

- Gallwey, J., Robiati, C., Coggan, J., Vogt, D. and Eyre, M. (2020), "A Sentinel-2 based multispectral convolutional neural network for detecting artisanal small-scale mining in Ghana: Applying deep learning to shallow mining", *Remote Sensing of Environment*, Vol. 248, p. 111970, doi: 10.1016/j.rse.2020.111970.
- Kozińska, P. and Górniak-Zimroz, J. (2021), "A review of methods in the field of detecting illegal open-pit mining activities", *IOP Conference Series: Earth and Environmental Science*, Vol. 942 No. 1, p. 012027, doi: 10.1088/1755-1315/942/1/012027.
- Mantey, S. and Otoo, E.K. (2020), "Assessing Activities of Illegal Mining in the Apamprama Forest Reserve of Ghana using Unmanned Aerial Vehicle (UAV)".
- Matingo, K. (2023), "Detecting Illegal Mining Activities in Zimbabwe through Earth Observation: A Case of Beitbridge District in Zimbabwe", In Review, 20 July, doi: 10.21203/rs.3.rs-3175436/v1.
- Mhangara, P., Tsoeleng, L.T. and Mapurisa, W. (2020), "Monitoring the development of artisanal mines in South Africa", *Journal of the Southern African Institute of Mining and Metallurgy*, Vol. 120 No. 4, doi: 10.17159/2411-9717/938/2020.
- Moomen, A.-W., Lacroix, P., Benvenuti, A., Planque, M., Piller, T., Davis, K., Miranda, M., *et al.* (2022), "Assessing the Applications of Earth Observation Data for Monitoring Artisanal and Small-Scale Gold Mining (ASGM) in Developing Countries", *Remote Sensing*, Vol. 14 No. 13, p. 2971, doi: 10.3390/rs14132971.
- Musiąlek, M. and Maksymowicz, M. (2025), "Remote sensing in mining: a brief overview and examples", *Górnictwo Odkrywkowe*, Vol. LXV No. 2, pp. 4–14, doi: 10.5604/01.3001.0055.0491.
- Myroniuk, V., Bilous, A., Khan, Y., Terentiev, A., Kravets, P., Kovalevskyi, S. and See, L. (2020), "Tracking Rates of Forest Disturbance and Associated Carbon Loss in Areas of Illegal Amber Mining in Ukraine Using Landsat Time Series", *Remote Sensing*, Vol. 12 No. 14, p. 2235, doi: 10.3390/rs12142235.
- Nursamsi, I., Phinn, S.R., Levin, N., Luskin, M.S. and Sonter, L.J. (2024), "Remote sensing of artisanal and small-scale mining: A review of scalable mapping approaches", *Science of The Total Environment*, Vol. 951, p. 175761, doi: <https://doi.org/10.1016/j.scitotenv.2024.175761>.
- Shivashankar, K., Hajj, G.S.A. and Martini, A. (2025), "Scalability and Maintainability Challenges and Solutions in Machine Learning: Systematic Literature Review", arXiv, 15 April, doi: 10.48550/arXiv.2504.11079.
- Snapir, B., Simms, D.M. and Waine, T.W. (2017), "Mapping the expansion of galamsey gold mines in the cocoa growing area of Ghana using optical remote sensing", *International Journal of Applied Earth Observation and Geoinformation*, Vol. 58, pp. 225–233, doi: 10.1016/j.jag.2017.02.009.

- Wang, S., Lu, X., Chen, Z., Zhang, G., Ma, T., Jia, P. and Li, B. (2020), "Evaluating the Feasibility of Illegal Open-Pit Mining Identification Using InSAR Coherence", *Remote Sensing*, Vol. 12 No. 3, p. 367, doi: 10.3390/rs12030367.
- Woldai, T. (n.d.). "Application of Remotely Sensed Data and GIS in Assessing the Impact of Mining Activities on the Environment".

## **BIOGRAPHICAL NOTES**

### **CONTACTS**

Dr Richmond Akwasi Nsiah  
University of Mines and Technology  
P. O. Box, Tarkwa, Ghana  
[ransiah@umat.edu.gh](mailto:ransiah@umat.edu.gh)  
[www.umat.edu.gh](http://www.umat.edu.gh)

Prof. Prosper Basommi Laari  
SD Dombo University of Business and Integrated Development Studies  
P. O. Box, X, Wa, Ghana  
[pbasomni@uds.edu.gh](mailto:pbasomni@uds.edu.gh)  
[www.uds.edu.gh](http://www.uds.edu.gh)

Prof. Qinfeng Guan  
China University of Geosciences  
Wuhan, China  
[guangf@cug.edu.cn](mailto:guangf@cug.edu.cn)  
[grzy.cug.edu.cn](http://grzy.cug.edu.cn)